

Study of the Effect of Inhibitors Solutions on the Chemical Composition of Waxes by Rheology Tests and High Resolution Mass Spectrometry

Lindamara M. Souza,^a Samantha R. C. Silva,^a Paulo R. Filgueiras,^a
Francine D. dos Santos,^a Géssica A. Vasconcelos,^b Valdemar Lacerda Jr.,^b *^a
Boniek G. Vaz^b and Wanderson Romão^b *^{a,c}

^aLaboratório de Petroleômica e Forense, Departamento de Química,
Universidade Federal do Espírito Santo, 29075-910 Vitória-ES, Brazil

^bInstituto de Química, Universidade Federal de Goiás, 74001-970 Goiânia-GO, Brazil

^cInstituto Federal de Educação, Ciência e Tecnologia do Espírito Santo,
29106-010 Vila Velha-ES, Brazil

Wax deposit is of a great concern in the petroleum industry and causes partial or total blockage of the pipelines. In this work, four Brazilian crude oils (P1-P4) and five inhibitors solutions (I1-I5) were used associating rheology results to understand, at a molecular level, the characteristics of the saturated fractions by high-resolution mass spectrometry (Orbitrap coupled to atmospheric pressure chemical ionization (APCI) source) and two-dimensional gas chromatography coupled to mass spectrometry (GC × GC-MS). The effectiveness of wax inhibitors can be demonstrated by the viscosity decrement. The characterization of the saturated fractions by GC × GC-MS and high resolution mass spectrometry showed that is possible to conclude that inhibitor I1 favored the inhibition process of paraffins when oils have a smaller and monocyclic saturated chain hydrocarbon (HC) profiles, whereas for oils with larger amounts of polycyclic chain HCs, the inhibitor I4 appeared to be the alternative.

Keywords: mass spectrometry, APCI, hydrocarbon, wax, rheology

Introduction

Petroleum is a complex mixture containing thousands of individual components, consisting predominantly of hydrocarbons (HCs), and in minor proportion, HC compounds containing heteroatoms, such as oxygen, nitrogen, and sulfur.^{1,2} In this context, petroleum waxes are mixtures of long chains of HCs containing carbon numbers (CN) ranging from C₁₈ to C₆₅.¹ In oil, they are present as *n*-alkanes (alicyclic), cycloparaffins (or cyclic aliphatic), and branched hydrocarbons (isoparaffins). For deposition behavior, *n*-alkanes are flexible HCs and tend to precipitate, while isoparaffins tend to retard the formation of crystallization nuclei, producing unstable solids. Contrarily, cycloalkanes tend to disturb or interrupt the nucleation and growth of wax deposits. The solubility of the waxes in crude oil is reduced as the temperature decreases, and deposits may occur on colder surfaces. Waxes crystallize when the wax appearance temperature

(WAT) is reached, and therefore, WAT can be defined as the highest temperature at which the first wax crystal forms when the oil is cooled.¹

The formation of deposits poses a problem for the petroleum industry, as they can cause interruptions or slow down the production. The deposition process can occur in the form of hydrates, asphaltenes, stains, and sands. Therefore, the wax deposit is extensively studied, being a complex and expensive problem, due to possible production stoppages.^{1,3,4}

Molecular diffusion is the preferred mechanism to explain the formation of wax deposits.⁵ Among the factors that contribute to this phenomenon are: the pour point, thermal history, oil composition, CN distribution of HCs, water-oil ratio, pressure, and the shear rate of oils.^{1,6} In addition to impurities, such as asphaltenes, clay, and corrosion, products can also act as nucleating agents for wax precipitation. Aromatic components, resins, naphthenes, and asphaltenes influence the crystallization kinetics and the solid-liquid equilibrium of *n*-alkane waxes of crude oil. Asphaltenes may act by reducing the formation

*e-mail: vljuniorqui@gmail.com; wandersonromao@gmail.com

barrier of the critical nuclei of wax but may also act to prevent or block the deposition of waxes. The form of action of asphaltenes depends mainly on its concentration and size.

There are several preventive and corrective methods to control wax deposition, such as, thermal insulated ducts, chemical inhibitors, heated solvents, the use of thermochemical reactions, and mechanical removal (pigging).⁷ The selection of the method depends on the characteristics of the deposit, and in accordance with the purpose to prevent or remedy the wax deposit.⁸ Chemical inhibitors have a lower cost when compared to other methods, and therefore, are recommended most often for the prevention of deposits.⁸ In this sense, cold-finger tests are commonly used to select the inhibitor.⁹

According to dos Santos *et al.*,³ a static cold-finger simulator can determine the critical temperature and deposition thickness of the waxes, helping in the prediction of the deposition of paraffins. In 2005, Jennings and Weispfennig¹⁰ evaluated the effect of temperature and shear rate on wax deposits obtained with a cold-finger simulator from Gulf of Mexico crude oils. The authors observed that the raise in the shear rate promotes an increase in the wax content of the deposit and the total amount of deposited wax increased when higher temperature difference between the oil and the cold surface was observed.¹⁰

The determination of the wax content, in this work, was executed by quantifying the peaks of *n*-alkanes detected by high temperature gas chromatography (HTGC). Similar results were observed in 2006 by Jennings and Weispfennig.¹¹ They studied four oils from the Gulf of Mexico, testing inhibitors and evaluating the shear rate. They concluded that the increase of the shear rate favors the inhibition of the amount of wax deposited. Hoffmann and Amundsen⁹ studied the influence of a wax inhibitor on the properties of the fluid and the deposit, determining the optimal concentration of the inhibitor. For this, they varied the inhibitor concentration from 0 to 500 mg L⁻¹, monitoring properties such as viscosity, WAT, wax content, and the wax solubility curve.

The wax analysis in the crude oil can be carried out with prior separation into fractions. The fractionation into saturated, aromatic, and polar (resins and asphaltenes), known as SAP method, is an alternative.^{2,12} Subsequently, the fractions can be analyzed without damage to the equipment, for example, gas chromatographic. The characterization of the samples can be performed by two-dimensional gas chromatography coupled to mass spectrometry (GC × GC-MS).¹³⁻¹⁵ This technique provides information about the number of carbons and the HC classes.¹⁶ In addition, the use of two chromatographic columns, with orthogonal separation mechanism, improves the selectivity, useful for complex samples.¹⁷

The information is given by HC classes highlighting the *n*-alkanes or *n*-paraffins, branched alkanes or iso-paraffins, alkenes or olefins, branched alkenes or iso-olefins, cycloalkanes or naphthenes, cycloalkenes, monocyclic, bicyclic, and tricyclic aromatics, and compounds with heteroatoms. Other advantages of the GC × GC-MS are the structural organization of the contour maps, besides the high-resolution and sensitivity when compared to the one-dimensional chromatography.¹⁷

High-resolution mass spectrometry (HRMS) is a consolidated analytic technique in petroleomics, presenting a greater contribution in the elucidation of the components present in saturated fractions with higher CNs.¹⁸ Furthermore, HRMS establishes information regarding the elemental composition (C_cH_hN_nO_oS_s) and the isotopic profile, which allows the identification of heteroatoms and double bond equivalent (DBE) that describes molecular aromaticity,¹⁹⁻²¹ molar mass distribution (M_w), and others.

The main obstacle in the analysis of wax deposits by HRMS was their ionization. In 2015, Tose *et al.*¹⁸ were able to analyze wax samples by Fourier-transform ion cyclotron resonance mass spectrometry (FT-ICR MS) using atmospheric pressure chemical ionization (APCI). For this, they used solvents with small CN (pentane, hexane, cyclohexane, heptane, and isooctane), identifying isooctane as the best solvent and reagent to promote paraffin ionization. In 2018, Souza *et al.*²² optimized APCI ionization, comparing the ionization efficiency using different nebulization gases (synthetic air, nitrogen (N₂), and helium (He)). They found that He is the best nebulizer gas for wax analysis.

In this work, four crude oils and five wax inhibitors (I1-I5) solutions were used in an attempt to associate the results obtained by rheology tests with the characteristics of their saturated fractions. High-resolution mass spectrometer (Q-Exactive Orbitrap MS) and a comprehensive two-dimensional gas chromatography coupled to mass spectrometry with a quadrupole-type analyzer (GC × GC-qMS) were used to understand the effect of inhibitors solutions on the chemical composition of petroleum waxes.

Experimental

Reagents and samples

Four oils from different wells (named P1, P2, P3, and P4) were studied. The properties of the oils characterized were density, water content, and pour point, Table 1.

Density was determined according to ASTM D7042 (2004)²³ using a digital densimeter, DMA 5000 (Anton

Table 1. Physicochemical properties of crude oils (P1-P4)

Crude oil	Density (293 K) / (g cm ⁻³)	API / degree	Pour point / K	Water content / wt. %
P1	0.868	30.7	258	0.280
P2	0.857	32.7	255	0.430
P3	0.860	32.4	270	0.070
P4	0.884	27.9	258	0.250

API: American Petroleum Institute.

Paar), and the measurements were obtained at 20 °C. To determine the water content of the oil samples, the Karl Fischer method by potentiometric titration was used with an automatic potentiometer 836 (Metrohm), according to ASTM D4377.²⁴ Pour point measurements were performed using automatic equipment PCA-70X.

Four saturated hydrocarbon fractions (SAT_P1-SAT_P4) of crude oils P1-P4, were obtained by the fractionation method of the crude oil that separates SAP.^{2,12} The method of SAP separation was done as reported in the literature.^{2,18} The percentages of saturated fractions (from SAT_P1 to SAT_P4) produced were equal to 60.3 ± 6.5, 73.7 ± 1.8, 56.7 ± 1.9, and 58.1 ± 2.6 wt.%, respectively. Isooctane was purchased by Vetec Química Fina Ltd., Duque de Caxias, Brazil, and used in the paraffin solution preparation and as an APCI reagent.

Inhibitors assessment

Rheology

Analyses were performed on the Anton Paar Physica MCR-301 rheometer with a CC-10 sensor. The oil was preheated to 80 °C. Tests were performed with the original samples (crude oils P1, P2, P3, and P4) and inhibited oils at the same concentrations, 1000 mg L⁻¹. All conditions and concentrations of the inhibitors are described in Table 2. The rheological measurements were performed at a rate of 10 and 120 s⁻¹, with a temperature ramp of 1 °C min⁻¹, ranging from 60 to 4 °C (333 to 277 K). The curves obtained were overlapped to compare the results. The performance of the wax inhibitor can be verified by the profile of the curves in the temperature range below WAT.

APCI(+)-MS

Orbitrap

Paraffin samples were analyzed by Q-Exactive Orbitrap MS (Thermo Fisher Scientific, Germany)²⁵ equipped with a commercial APCI source set to operate over *m/z* 200-1500.^{18,22,26} Samples of paraffins were analyzed using a positive ionization mode, APCI(+).

The preparation of the four solutions containing saturated fractions (SAT_P1-SAT_P4) and of the APCI(+) source

Table 2. Viscosity values at 278 K for the shear rates of 10 and 120 s⁻¹ for oils P1-P4 with and without inhibitors (I1-I5)

Petroleum	Concentration of inhibitor / (mg L ⁻¹)	Inhibitor	Viscosity at 278 K in the rate of 10 s ⁻¹ / cP	Intersection in the rate of 10 s ⁻¹		Viscosity at 278 K in the rate of 120 s ⁻¹ / cP	Intersection in the rate of 120 s ⁻¹	
				K	cP		K	cP
P1	–	without	222.0	287.9	11.70	226.0	288.8	31.16
	1000	I1	265.0	290.8	6.612	167.0	291.8	17.37
	1000	I2	215.5	290.4	16.17	191.0	290.4	22.68
P2	–	without	585.5	292.9	15.58	204.0	292.5	17.35
	1000	I1	239.0	293.5	16.01	116.5	293.1	17.75
	1000	I2	129.5	295.1	24.55	57.95	300.8	12.74
P3	–	without	57.00	289.9	17.46	39.05	290.2	15.63
	1000	I1	156.5	291.2	30.29	45.70	291.1	17.97
	1000	I2	60.30	290.6	17.56	56.10	290.8	22.25
P4	–	without	1094	293.4	62.44	855.5	291.3	92.68
	1000	I1	1165	293.5	60.25	417.0	293.4	61.46
	5000	I1	775.0	293.1	63.23	436.0	293.4	64.69
	1000	I2	3065	296.4	98.76	930.0	294.8	117.9
	2000	I3	724.5	290.2	61.41	384.0	291.1	89.32
	5000	I3	611.0	289.8	68.07	591.5	292.0	133.0
	2000	I4	316.0	293.8	62.06	222.5	292.3	62.61
2000	I5	504.0	292.1	86.53	184.5	291.4	55.18	

conditions were followed as reported by Tose *et al.*¹⁸ and Souza *et al.*²² The resulting solution was sonicated for 10 min at 40 °C and directly infused in an APCI(+) source using a flow rate of 40 $\mu\text{L min}^{-1}$. The APCI(+) source conditions were: sheath gas of 40 (arbitrary units), auxiliary gas of 20 (arbitrary units), temperature at 275 °C, capillary voltage of 4.0 kV, and S-Lens of 100. Each spectrum was acquired by accumulating 50 scans using 10 micro scans, totaling 500 scans. All mass spectra were externally calibrated using an LTQ Orbitrap Velos solution, which covers m/z ranging from 50 to 2000. The mass resolving power employed was $m / \Delta m_{50\%} = 140,000$ (in which $\Delta m_{50\%}$ is the full peak width at half-maximum peak height of m/z 200) and mass accuracy of < 1 ppm provided the unambiguous molecular formula assignments for singly charged molecular ions. Data were processed using XCalibur and the molecular formulas were assigned on the Composer software (Sierra Analytics, Modesto, CA, USA).²⁷⁻³²

GC \times GC-qMS

The four saturated fractions (denominated by fractions SAT_P1-SAT_P4) were prepared in a concentration of 500 mg L^{-1} of dichloromethane and analyzed by GC \times GC-qMS (Shimadzu QP2010 Ultra System) with a ZX1-GC \times GC modulator (Zoex, Houston, TX, USA). The chromatographic separation was performed as described by Soares *et al.*¹³ and Coutinho *et al.*¹⁴ The mass range was examined from 50 to 600 Da, with a modulation period of 6 s. GC Image software³³ was used for the identification of compounds.

Results and Discussion

Rheology results

In 2005, Jennings and Weispfennig¹⁰ studied the effect of temperature and shear stress. According to the authors, to have wax deposition occur in the cold-finger tests, there must be a temperature difference between the crude oil and the deposition surface. Moreover, the increase of temperature difference causes an increase in the thermodynamics of the deposition driving force, consequently, a larger deposition of wax occurs. However, the higher the temperature variation between the cold-finger and the oil favors a greater amount of crude oil occluded in the wax deposit.¹⁰ In 2006, the same authors used four oils from the Gulf of Mexico to perform the test with inhibitors and evaluated the effect of shear rate. They concluded that there was a general trend between the improved performance of the wax inhibitor and an increase in shear force. This trend was based on the inhibition amount of wax

in the deposits and the free surface area (without deposit) of the cold-finger.¹¹ It is important to note that the rotation of the cold-finger allows the shear to occur at the deposition surface, similar to that happening in the flow of the pipes. However, it is not yet possible to simulate the shear strength in the cold-finger equipment.

Wax precipitation may also be followed by an increase in apparent viscosity, which may lead to loss of flowability. Moreover, this property is associated with the temperature, thus, affecting wax deposition events. The WAT can be determined from the graph of viscosity *versus* temperature obtained by rheological measurements at the point where the linearity deviation occurs. This point can be determined by the intersection of two parallel lines (trend lines) used to evaluate the efficiency of the inhibitor. The presence of the inhibitors caused deviations in the curves in relation to the pure crude oil (blank) at temperatures of 275 to 295 K. Conversely, WAT values remained practically constant in the presence of inhibitors.

It was expected that the decrease of temperature increases the viscosity, and this result can be observed in all cases of the temperature *versus* viscosity curves, Figures 1a-1e and 2a-2e, obtained in shear rates at 10 and 120 s^{-1} , respectively. Figures 1a-1d and 2a-2d present rheology measurements for petroleum samples P1 (1a, 2a), P2 (1b, 2b), P3 (1c, 2c), and P4 (1d, 2d) (with and without inhibitors I1 and I2 at 1000 mg L^{-1} and shear rate at 10 and 120 s^{-1} , respectively). Figures 1e and 2e present rheology measurements for the oil P4 in the presence of all inhibitors ([I1] = 1000 mg L^{-1} ; [I2] = 1000 mg L^{-1} ; [I3] = 2000 mg L^{-1} ; [I4] = 2000 mg L^{-1} ; [I5] = 2000 mg L^{-1} ; [I1] = 5000 mg L^{-1} ; and [I3] = 5000 mg L^{-1}) obtained in shear rates of 10 and 120 s^{-1} , respectively.

From the results of the rheological measurements, such as those presented in Figures 1 and 2, it was possible to construct Table 2, which contains viscosity values at 278 K at shear rates of 10 and 120 s^{-1} , WAT, and their respective viscosity. When comparing the viscosity values at 278 K (the two shear rates, Figures 1a and 2a) for the crude oil P1, the viscosity was practically unchanged. Conversely, the viscosity of the oil P1 doped with the inhibitors I1 and I2 showed a change in the profile of the curve in the two shear rates studied, especially after WAT ($T \leq 288$ K). For example, at 278 K, when comparing the viscosity value at rates of 10 s^{-1} (Figure 1a), it is possible to observe a variation of +43 cP relative to the crude oil P1 when inhibitor I1 was used, while the inhibitor I2 caused a variation of -7 cP. It is uninteresting that an inhibitor changes the viscosity values in the same temperature range because this shows a deviation from the Newtonian behavior and can cause problems for injection by the umbilical system.

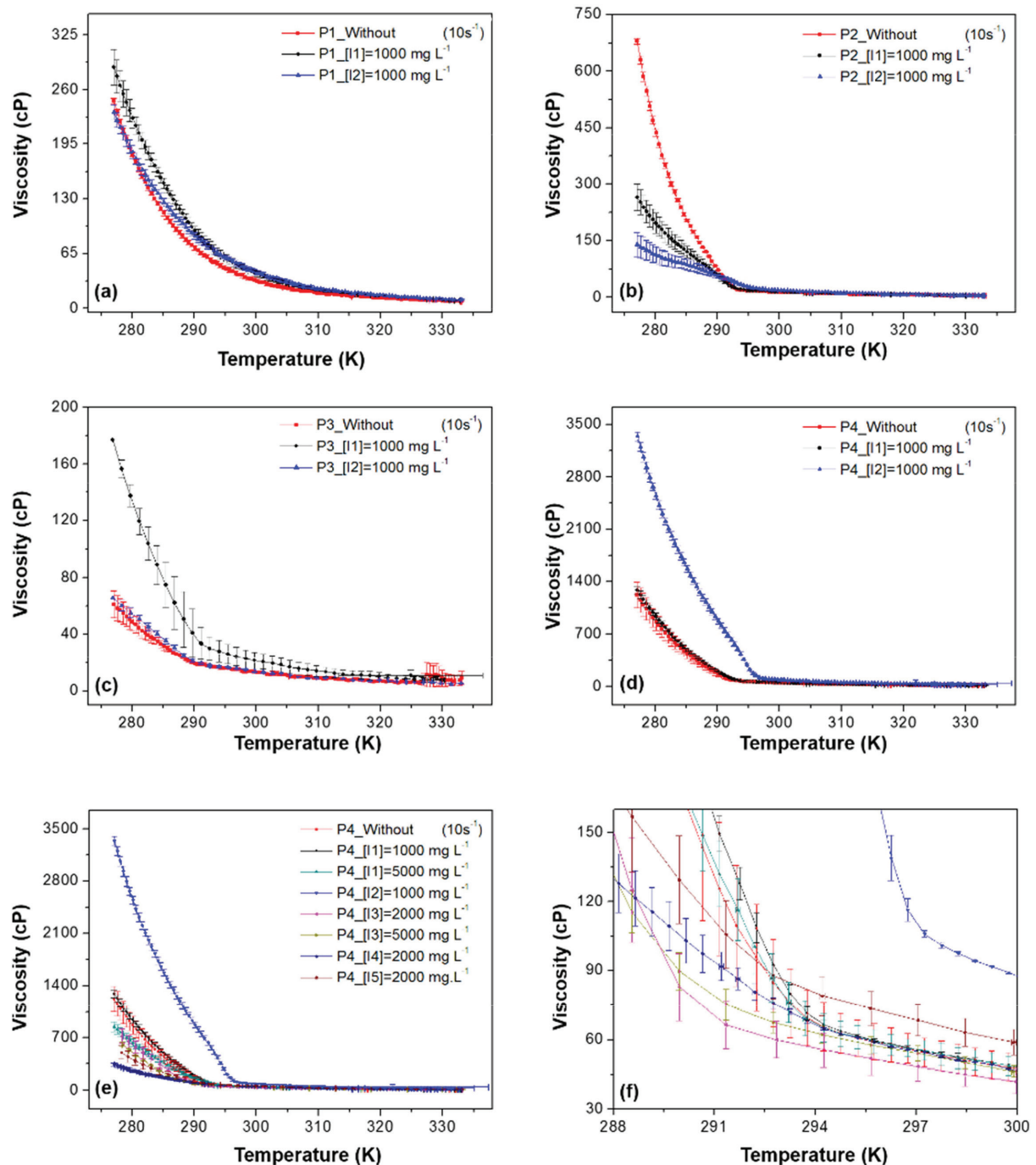


Figure 1. Rheology results for crude oil samples P1 (a); P2 (b); P3 (c) and P4 (d) without and with inhibitor ($[I1] = [I2] = 1000 \text{ mg L}^{-1}$) at shear rate of 10 s^{-1} ; (e) rheology measurements for oil P4 (blank, and with inhibitors ($[I1] = [I2] = 1000 \text{ mg L}^{-1}$; $[I3] = 2000 \text{ mg L}^{-1}$; $[I4] = 2000 \text{ mg L}^{-1}$; $[I5] = 2000 \text{ mg L}^{-1}$; $[I1] = 5000 \text{ mg L}^{-1}$; and $[I3] = 5000 \text{ mg L}^{-1}$), and (f) an extension of Figure 1e.

For the oil P1, the inhibitor I2 presented a smaller variation of its viscosity as a function of the shear rate, being the most recommended for application in the petrochemical industry. Now, considering the WAT results for the same oil doped with the inhibitors (I1 and I2), it is possible to note that they remain constant, varying only in the range of 288 to 291 K for the shear rate 10 s^{-1} (Figure 1a) and in the range from 289 to 292 K for the shear rate 120 s^{-1} (Figure 2a). But

when comparing the influence of the inhibitor on the viscosity of the WAT, inhibitor I1 reduced the viscosity values nearly in half ($v_{10 \text{ s}^{-1}} = 11.7 \rightarrow 6.6 \text{ cP}$ and $v_{120 \text{ s}^{-1}} = 31.6 \rightarrow 17.4 \text{ cP}$), while when using inhibitor I2, the viscosity at the shear rate 10 s^{-1} increased (16.2 cP). Therefore, inhibitor I1 was able to reduce the oil viscosity independent of the shear rate. This behavior can be used to explain the better efficiency of this inhibitor over inhibitor I2.

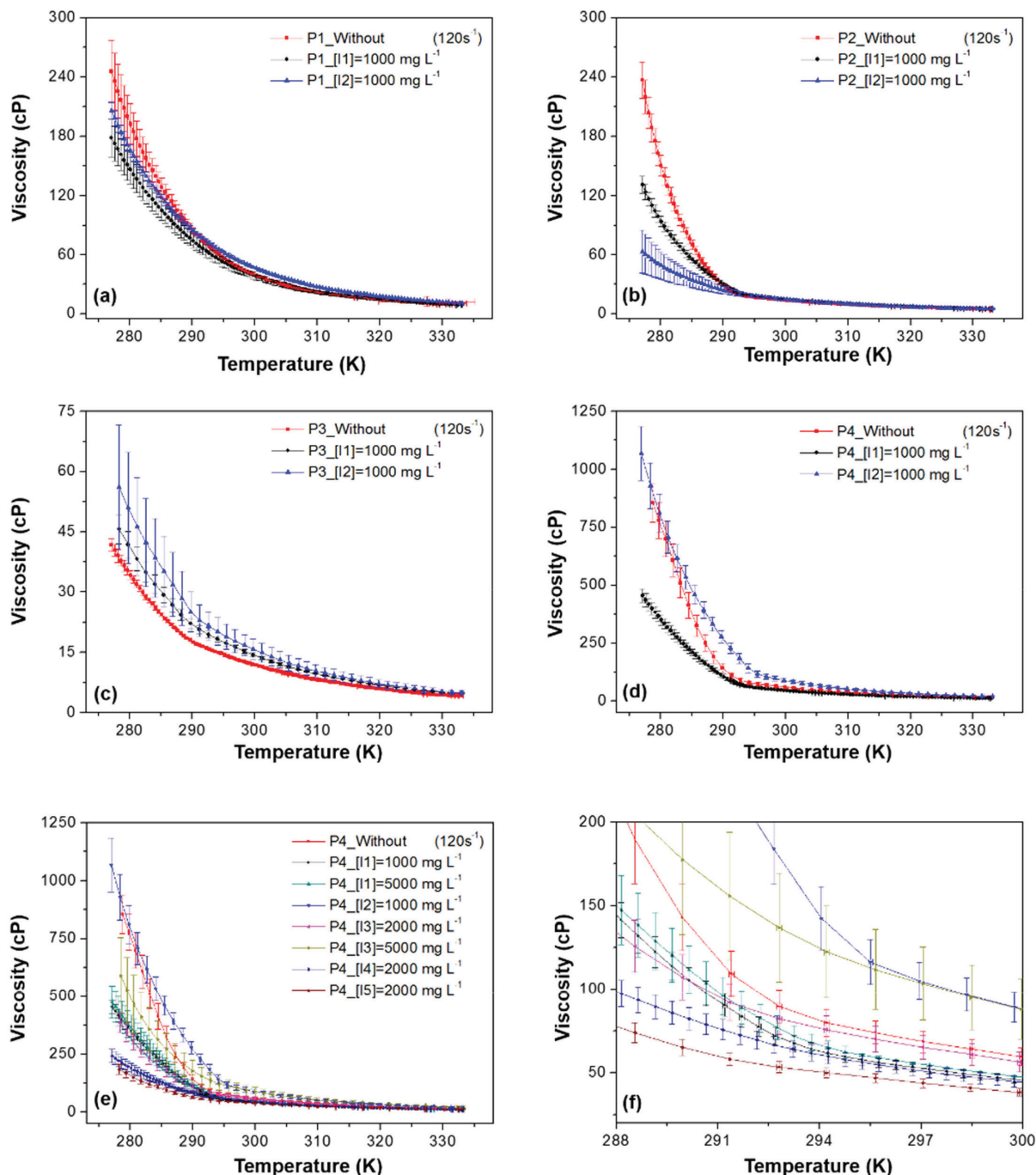


Figure 2. Rheology measurements for crude oils P1 (a); P2 (b); P3 (c) and P4 (d) (blank, and with inhibitors I1 and I2 at 1000 mg L^{-1}) at shear rate of 120 s^{-1} ; (e) rheology measurements for crude oil P4 (blank, and with inhibitors ([I1] = 1000 mg L^{-1} ; [I2] = 1000 mg L^{-1} ; [I3] = 2000 mg L^{-1} ; [I4] = 2000 mg L^{-1} ; [I5] = 2000 mg L^{-1} ; [I1] = 5000 mg L^{-1} and [I3] = 5000 mg L^{-1}) and (f) an extension of Figure 2e.

Observing the rheological profile of the crude oil P2, the viscosity of the oil P2 was reduced at both shear rates when it was doped with inhibitors I1 and I2 (Figures 1b and 2b). Conversely, when using inhibitor I2, a more pronounced increase in WAT was observed ($T_{\text{WAT}} = 8 \text{ K}$, $292 \rightarrow 300 \text{ K}$, at shear rate 120 s^{-1}) comparing with inhibitor I1, which remained practically constant (Figure 2b). This is because this inhibitor is responsible for more efficiently

reducing the viscosity at temperatures lower than WAT (i.e., $< 292 \text{ K}$). The oil P2 is the oil with the highest saturates content among the studied oils, “Reagents and samples” sub-section, followed by the oils P1, P4, and P3, respectively, explaining why, at temperatures below of WAT, the viscosity values of this oil were greatly affected by the presence of inhibitors I1 and I2.

Reading the rheological profile of the oil P3 in the

viscosity *versus* temperature curve (Figures 1c and 2c), it was observed that inhibitors I1 and I2 increased the viscosity of the oil throughout the temperature range studied (Table 2). While the viscosity of the oil P3 was 17.5 and 15.6 cP at shear rates 10 and 120 s⁻¹, respectively, inhibitor I1 caused an increase of 30.3 and 18.0 cP for the same shear rates. Analogous results were observed for inhibitor I2. These results are an indicative that the increase significance of viscosity as a function of temperature proves that the inhibitor performance in the prevention of wax precipitation is inefficient.

Finally, for the oil P4, only the inhibitor I4 caused a viscosity reduction in WAT at both shear rates (Figures 1d and 2d) studied in relation to its blank (oil P4 without inhibitor), with a viscosity reduction at the shear rate of 120 s⁻¹ (92.7 → 62.6 cP). Additionally, this inhibitor reduced the viscosity at 278 K for the shear rates of 10 and 120 s⁻¹ (1094 → 316.0 cP and 855.5 → 222.5 cP,

respectively). These results suggest that the inhibitor I4 can have a higher efficiency on the wax deposit reduction.

Figures 1f and 2f show an extension on the WAT region for the oil P4 with the five inhibitors. In the curve at shear rate of 10 s⁻¹, inhibitors I3 and I4 decreased the WAT, Figure 1f. This occurs because oil P4 containing inhibitor I3 showed higher viscosity values (611 and 591.5 cP) than with inhibitor I4 (316 and 222.5 cP) at both shear rates studied. The efficiency of the inhibitors was associated with a simultaneous reduction of viscosity at 278 K and WAT in relation to crude oil without an inhibitor.

APCI(+)-MS and GC × GC-qMS

To better understand the results obtained in the inhibition tests, the saturated fractions of the oils P1, P2, P3, and P4, called SAT_P1-SAT_P4, were analyzed by GC × GC-qMS (Figure 3), and APCI(+) Q-Exactive Orbitrap MS (Figures 4-6).

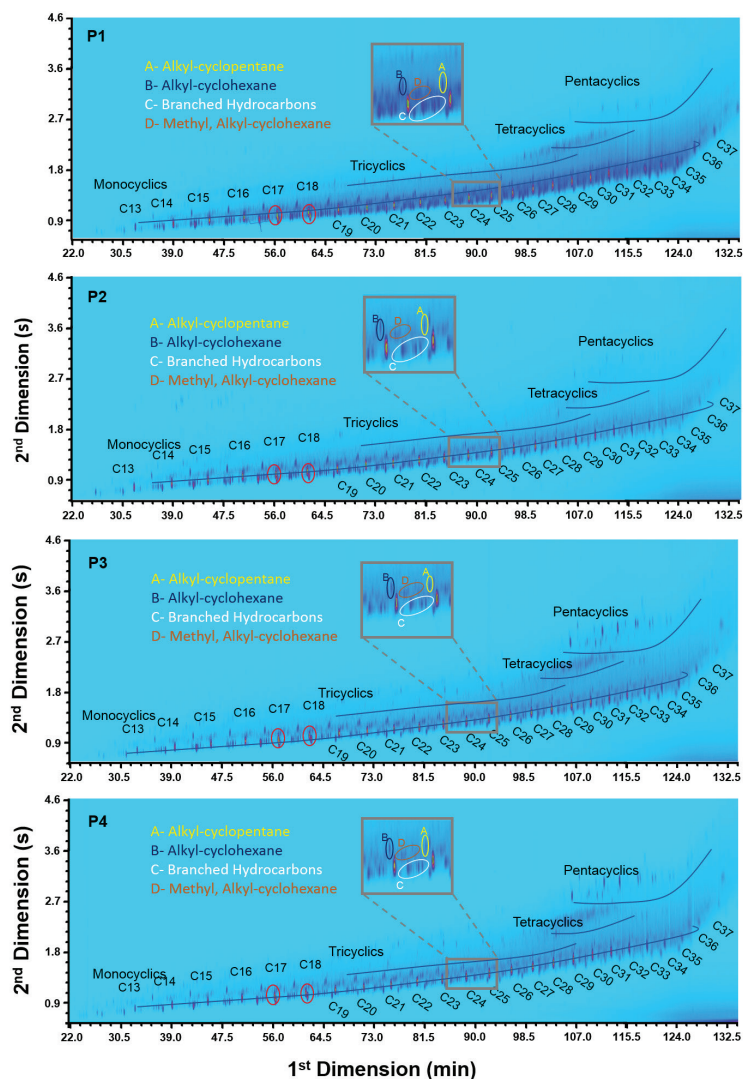


Figure 3. GC × GC-qMS chromatograms of the four saturated fractions: (a) SAT_P1; (b) SAT_P2; (c) SAT_P3 and (d) SAT_P4.

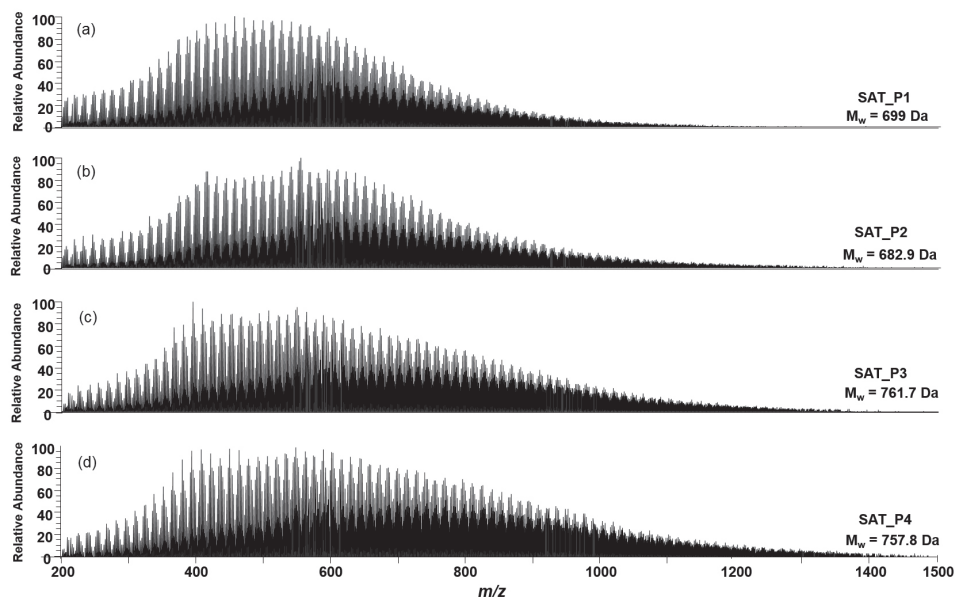


Figure 4. APCI(+)-Q-Exactive Orbitrap MS for the saturated fractions (a) SAT_P1; (b) SAT_P2; (c) SAT_P3 and (d) SAT_P4.



Figure 5. (a) Class distribution plot for the samples SAT_P1, SAT_P2, SAT_P3 and SAT_P4; and DBE versus intensity plots for the samples (b) SAT_P1; (c) SAT_P2; (d) SAT_P3 and (e) SAT_P4 from APCI(+)-Orbitrap MS results.

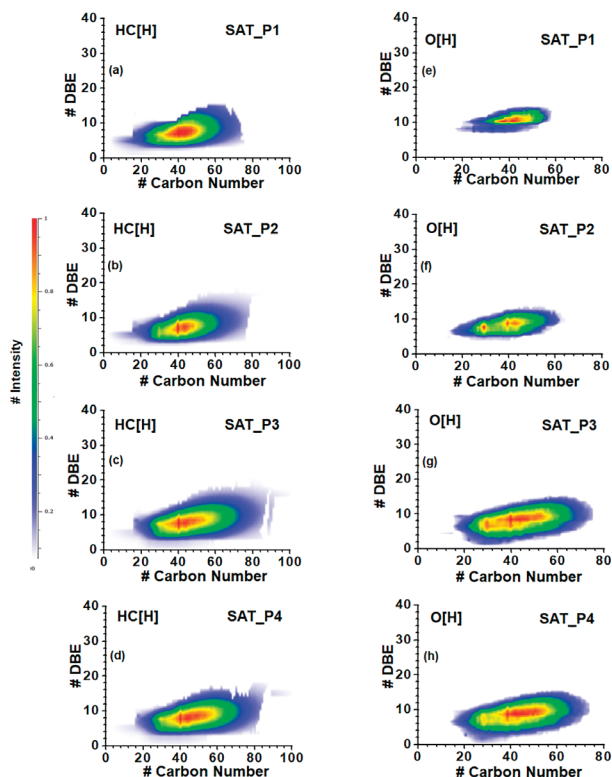


Figure 6. DBE *versus* carbon number (CN) plot for the HC[H] and O[H] classes of the saturated fractions (a, e) SAT_P1, (b, f) SAT_P2, (c, g) SAT_P3 and (d, h) SAT_P4.

GC \times GC-qMS is a novel technique and has been applied in the oil fields.^{16,34,35} This technique differentiates HCs into saturated, branched, cyclic, and aromatic, for example. The GC \times GC-qMS results are presented in Figures 3a-3d and elucidate the molecular composition of the saturated fractions of the oils P1-P4, classifying them as linear, branched, and cyclic; whereas, for linear HCs, a distribution of CNs ranging from C₁₃ to C₃₇ was observed. Moreover, other HC groups have been detected, such as alkyl-cyclopentane (A), alkyl-cyclohexane (B), branched HCs (C), and methyl, alkyl-cyclohexane (D).

It should be noted that the samples of saturated HCs from oils P1 and P2 showed higher intensity for compounds containing linear and monocyclic chains (alkyl-cyclopentanes, alkyl-cyclohexane, branched hydrocarbons, methyl, and alkyl-cyclohexane), than of polycyclic compounds (tricyclic, tetracyclic and pentacyclic). The opposite was observed for the saturated fractions from the oils P3 and P4. Combining these results with those observed in the inhibitor test (Table 2), it can be concluded that the inhibitor I1 was efficient for the saturated fractions that showed a higher intensity of compounds containing linear and monocyclic HCs chains, whereas, the inhibitor I4 was efficient for samples with saturated HCs fraction that shows a higher intensity

of polycyclic compounds (tricyclic, tetracyclic, and pentacyclic compounds).

Figures 4a-4d show the chemical profile of APCI(+) Orbitrap MS for the saturated fractions SAT_P1-SAT_P4 in the region of *m/z* 200-1500. APCI(+) Orbitrap MS data showed that *M_w* values obey the following order of magnitude: P3 (762 Da) > P4 (758 Da) > P1 (699 Da) > P2 (683 Da). Note that the higher values of *M_w* were associated with the petroleum which the inhibitor I1 showed no efficiency, as verified in rheology results (Table 2).

According to the rheology results, Table 2, it was expected that the profile of the waxes from the oils P1 and P2 would be similar. In addition, these oils have higher saturated contents, according to the data obtained by the SAP methodology. With APCI(+) Orbitrap MS data, it was possible to construct the class diagram, Figure 5a, and DBE *versus* intensity plots, Figures 5b-5e.

The HCs ionization using the APCI source occurred by gas phase reactions between molecules of the analyte, nebulizer gas, and solvent when subjected to corona discharge. As a result, ions detected are formed by the abstraction of hydrides [M - H]⁺, where M represents the HC molecules.^{18,22}

The graph of the class distribution, Figure 5a, which shows the HC[H] class as the most abundant, presented heteroatoms classes, such as O[H] and S[H]. The abundance of the HC[H] class was 82.3, 93.6, 89.3, and 90.2% for the samples SAT_P1, SAT_P2, SAT_P3, and SAT_P4, respectively. Therefore, sample SAT_P2 presented a higher abundance of HC[H] class between the samples, having the majority percentage of saturated HCs (74 wt.%). Souza *et al.*²² observed that using N₂ or synthetic air as reacting gas in the APCI source, a higher abundance of heteroatoms molecules was detected,²² thus, explaining the presence of the O[H] and S[H] classes.

DBE distribution, Figures 5b-5e, shows a wider distribution of HCs, HC[H] class, for the oils P3 and P4 (DBEs of 3-18 and 3-19, respectively), whereas a smaller amplitude of distribution was observed for oil P1 (DBE = 3-15) (Figures 5b-5e).

The DBE *versus* CN plots (Figures 6a-6h) for HC[H] and O[H] classes are conclusive to explain the inhibitor test results. Understanding the results for the HC[H] class (Figures 6a-6d), it is possible to ionize molecules with CN between C₄-C₈₀ for samples SAT_P1 and SAT_P2, with maximum distribution between C₃₀-C₅₀. Contrarily, the samples SAT_P3 and SAT_P4 presented higher HC distribution, varying from C₁₆ to C₁₀₀, with the maximum centered at C₃₀-C₆₀. Furthermore, the DBE *versus* CN plot for O[H] class (Figures 6e-6h) of the samples SAT_P3 and

SAT_P4 corroborate with the HC[H] class data, being also more abundant in these samples.

The DBE values $\neq 0$ indicate presence of unsaturated, cyclic, and/or aromatic HCs. Based on the GC \times GC-qMS results, the samples SAT_P3 and SAT_P4 showed molecules with higher DBEs, observed in Figure 3, with a greater number of compounds in the tetracyclic and pentacyclic regions. These results corroborate with the fact that inhibitors I1 and I2 were efficient for samples with lower intensities of polycyclic and aromatic HCs compounds. Conversely, the inhibitor I4 is more selective for saturated HCs fractions with higher distribution of CNs and DBEs.

Conclusions

The rheological tests showed that the efficiency of the inhibitor is mainly associated with the reduction of the viscosity in WAT. From the characterization of the saturated HCs fractions by HRMS and two-dimensional gas chromatography coupled to mass spectrometry, it can be concluded that inhibitor I1 favored the inhibition of oils with a saturated HCs profile containing smaller and monocyclic chains, whereas, an oil containing polycyclic chains needs a distinct inhibitor to avoid the wax deposition process. In this case, inhibitor I4 appeared to be the best alternative.

Acknowledgments

The authors thank CAPES, CNPq and FAPES for their financial support. The authors also thank the Núcleo de Competências em Química do Petróleo (UFES), coordinated by Prof Dr Eustaquio V. R. Castro, for the GC \times GC-qMS analyses.

References

1. Valinejad, R.; Nazar, A. R. S.; *Fuel* **2013**, *106*, 843.
2. Filgueiras, P. R.; Portela, N. A.; Silva, S. R.; Castro, E. V.; Oliveira, L. M.; Dias, J. C.; Neto, A. C.; Romão, W.; Poppi, R. J.; *Energy Fuels* **2016**, *30*, 1972.
3. dos Santos, J. D. S.; Fernandes, A. C.; Giulietti, M.; *J. Pet. Sci. Eng.* **2004**, *45*, 47.
4. Aiyejina, A.; Chakrabarti, D. P.; Pilgrim, A.; Sastry, M. K. S.; *Int. J. Multiphase Flow* **2011**, *37*, 671.
5. Quan, Q.; Gong, J.; Wang, W.; Gao, G.; *J. Pet. Sci. Eng.* **2015**, *130*, 1.
6. Guozhong, Z.; Gang, L.; *J. Pet. Sci. Eng.* **2010**, *70*, 1.
7. Rocha, N. O.; Gonzáles, G.; Vaitsman, D. S.; *Quim. Nova* **1998**, *21*, 11.
8. Lemos, B. C.; Gilles, V.; Gonçalves, G. R.; de Castro, E. V. R.; Delarmelina, M.; Carneiro, J. W. D. M.; Greco, S. J.; *Fuel* **2018**, *220*, 200.
9. Hoffmann, R.; Amundsen, L.; *J. Pet. Sci. Eng.* **2013**, *107*, 12.
10. Jennings, D. W.; Weispfennig, K.; *Energy Fuels* **2005**, *19*, 1376.
11. Jennings, D. W.; Weispfennig, K.; *Energy Fuels* **2006**, *20*, 2457.
12. Rodrigues, E. V.; Silva, S. R.; Romão, W.; Castro, E. V. R.; Filgueiras, P. R.; *Fuel* **2018**, *220*, 389.
13. Soares, R. F.; Pereira, R.; Silva, R. S. F.; Mogollon, L.; Azevedo, D. A.; *J. Braz. Chem. Soc.* **2013**, *24*, 1570.
14. Coutinho, D. M.; França, D.; Vanini, G.; Mendes, L. A. N.; Gomes, A. O.; Pereira, V. B.; Ávila, B. M.; Azevedo, D. A.; *Fuel* **2018**, *220*, 379.
15. Vanini, G.; Pereira, V. B.; Romão, W.; Gomes, A. O.; Oliveira, L. M. S.; Dias, J. C. M.; Azevedo, D. A.; *Microchem. J.* **2018**, *137*, 111.
16. Li, S.; Cao, J.; Hu, S.; *Fuel* **2015**, *158*, 191.
17. Von Mühlen, C.; Zini, C. A.; Caramão, E. B.; Marriott, P. J.; *Quim. Nova* **2006**, *29*, 765.
18. Tose, V. L.; Cardoso, F. M. R.; Fleming, F. P.; Vicente, M. A.; Silva, S. R. C.; Aquije, G. M. F. V.; Vaz, B. G.; Romão, W.; *Fuel* **2015**, *153*, 346.
19. Terra, L. A.; Filgueiras, P. R.; Tose, L. V.; Romão, W.; de Souza, D. D.; de Castro, E. V. R.; de Oliveira, M. S.; Dias, J. C.; Poppi, R. J.; *Analyst* **2014**, *139*, 4908.
20. Vaz, B. G.; Abdelnur, P. V.; Rocha, W. F.; Gomes, A. O.; Pereira, R. C.; *Energy Fuels* **2013**, *27*, 1873.
21. Marshall, A. G.; Rodgers, R. P.; *Acc. Chem. Res.* **2004**, *37*, 53.
22. Souza, L. M.; Tose, L. V.; Cardoso, F. M. R.; Fleming, F. P.; Pinto, F. E.; Kuster, R. M.; Filgueiras, P. R.; Vaz, B. G.; Romão, W.; *Fuel* **2018**, *225*, 632.
23. ASTM D7042: *Standard Test Method for Kinematics Viscosity in Crude Oil*, ASTM International, West Conshohocken, PA, 2004.
24. ASTM D4377: *Standard Test Method for Karl Fischer in Crude Oil*, ASTM International, West Conshohocken, PA, 2006.
25. Vasconcelos, G. A.; Pereira, R. C.; Santos, C. D. F.; Carvalho, V. V.; Tose, L. V.; Romão, W.; Vaz, B. G.; *Int. J. Mass Spectrom.* **2017**, *418*, 67.
26. Pereira, T. M. C.; Vanini, G.; Tose, L. V.; Cardoso, F. M. R.; Fleming, F. P.; Rosa, P. T. V.; Thompson, C. J.; Castro, E. V. R.; Vaz, B. G.; Romão, W.; *Fuel* **2014**, *131*, 49.
27. Zorzenão, P. C.; Mariath, R. M.; Pinto, F. E.; Tose, L. V.; Romão, W.; Santos, A. F.; Scheer, A. P.; Simon, S.; Sjöblom, J.; Yamamoto, C. I.; *J. Pet. Sci. Eng.* **2018**, *160*, 1.
28. Pinto, F. E.; Silva, C. F.; Tose, L. V.; Figueiredo, M. A.; Souza, W. C.; Vaz, B. G.; Romão, W.; *Energy Fuels* **2017**, *31*, 3454.
29. Carvalho, V. V.; Vasconcelos, G. A.; Tose, L. V.; Santos, H.; Cardoso, F. M. R.; Fleming, F. P.; Romão, W.; Vaz, B. G.; *Fuel* **2017**, *210*, 514.

30. Nascimento, P. T.; Santos, A. F.; Yamamoto, C. I.; Tose, L. V.; Barros, E. V.; Gonçalves, G. R.; Freitas, J. C.; Vaz, B. G.; Romão, W.; Scheer, A. P.; *Energy Fuels* **2016**, *30*, 5439.
31. Pinto, F. E.; Barros, E. V.; Tose, L. V.; Souza, L. M.; Terra, L. A.; Poppi, R. J.; Vaz, B. G.; Vasconcelos, G.; Subramanian, S.; Simon, S.; Sjöblom, J.; *Fuel* **2017**, *210*, 790.
32. Adermann, N.; Boggiano, J.; *Composer*, version 1.5.3; Sierra Analytics, Pasadena, CA, USA, 2016.
33. *GC Image software*, version 2.1b4; Zoex Corporation, Houston, TX, USA, 2001.
34. Lu, H.; Shi, Q.; Lu, J.; Sheng, G.; Peng, P. A.; Hsu, C. S.; *Energy Fuels* **2013**, *27*, 7245.
35. Silva, R. C.; Silva, R. S. F.; de Castro, E. V. R.; Peters, K. E.; Azevedo, D. A.; *Fuel* **2013**, *112*, 125.

Submitted: April 28, 2019

Published online: September 17, 2019

